Notices to investigation of symbiotic binaries V. Physical parameters derived from *UBV* magnitudes

Z. Cariková, A. Skopal

Astronomical Institute, Slovak Academy of Sciences, 059 60 Tatranská Lomnica, Slovakia

Received -; accepted -

Abstract

In the optical, the spectrum of symbiotic binaries consists of contributions from the cool giant, symbiotic nebula and the hot star. Strong emission lines are superposed on the continuum. In this paper we introduce a simple method to extract individual components of radiation from photometric *UBV* magnitudes. We applied the method to classical symbiotic stars AX Per, AG Dra, AG Peg and Z And, the symbiotic novae RR Tel and V1016 Cyg and the classical nova V1974 Cyg during its nebular phase. We estimated the electron temperature and emission measure of the nebula in these systems and the *V* magnitude of the giant in the symbiotic objects. Our results are in a good agreement with those obtained independently by a precious modelling the UV–IR SED.

Keywords: Stars: binaries: symbiotic; techniques: photometric
PACS: 97.30.Eh, 97.30.Qt, 97.80.Gm

1. Introduction

Symbiotic stars are long-period ($P_{orb} \sim 1-3$ years or more) interacting binary systems, which comprise a late-type giant (usually a red giant of the spectral type M) and a hot compact star, most probably a white dwarf. If the giant of the spectral type G or K is present, we call them 'yellow symbiotics'. During quiescent phases, the white dwarf accretes a fraction of the wind from the giant. Typical mass loss rate from the giant in the symbiotic binaries is of a few times $10^{-7}\,M_\odot\,\mathrm{yr}^{-1}$. The accretion process leads to heating up the white dwarf's surface to a very high temperature of $T_h \sim 10^5$ K, and increases its luminosity to $L_h \sim 10^2 - 10^4\,L_\odot$. Such the hot and luminous WD is capable of ionizing neutral wind particles of both the stars giving rise to a strong nebular radiation. During quiescent phases, the symbiotic nebula represents mostly the ionized part of the stellar wind from the giant. During active phases, the mass loss rate from the hot component increases, and can temporary exceed that from the giant. As a result, properties of the symbiotic nebula significantly change during the active phases.

Accordingly, the observed flux, F_λ (corrected for the interstellar extinction) is given by the superposition of three basic components of radiation – from the nebula, F_λ^{nebula}, the cool giant, F_λ^{giant}, and the hot stellar source, F_λ^{hot}, i.e.

$$F_\lambda = F_\lambda^{nebula} + F_\lambda^{giant} + F_\lambda^{hot}. \quad (1)$$

Contributions of the individual components of the radiation depend on the wavelength. The hot stellar source dominates the far-*UV* spectrum, while the nebula is usually dominant in the near-*UV*/*U* domain, and the cool giant (especially the red giant) dominates the near-*IR* spectral region. In the case of yellow symbiotics the contribution of the giant to the Johnson's *V* filter is very strong relatively to that from the nebula. However, contributions from different sources in a symbiotic system depend also on the level of the activity.

During active phases of symbiotic binaries with a high orbital inclination, we observe narrow minima in their light curves. They can be interpreted as eclipses of the hot object by the cool giant. This implies that during the activity the hot stellar source produces a dominant amount of its radiation within the optical region. It is believed that an optically thick disk is formed around the hot star at the orbital plane during active phases (see Skopal, 2005). Its relatively cool rim mimics a warm pseudophotosphere, while the circumstellar material above/below the disk can easily be ionized by its hot central part. Therefore the observed depths of the minima are partially filled in by the nebular radiation. Thus during the eclipses, the observed light consists of the contributions from the giant and the nebula. During quiescent phases the optical region is dominated by the extensive nebula, which thus prevents from observing eclipses. Corresponding colour indices are very different from those observed during active phases.

The aim of this paper is to propose a method of disentangling photometric *UBV* magnitudes of symbiotic stars into their components from contributing sources as given by Eq. (1). This means to determine physical parameters of their radiation. In particular, the electron temperature, T_e, and emission measure, EM, of the symbiotic nebula, and the brightness of the cool giant in the *V* passband (V^{giant}). We describe our method in the following section. First, we formulated some simplify-

Email addresses: zcarikova@ta3.sk (Z. Cariková), skopal@ta3.sk (A. Skopal)

ing assumptions (Sect. 2.1), and then we derived a system of equations, which relates theoretical properties of the radiative components to their observational characteristics (Sect. 2.4). In Sect. 3 we applied this approach to selected objects and compared the results with those achieved independently by another methods. Discussion and summary of the results are found in Sects. 4 and 5, respectively.

2. The method

2.1. Assumptions

In our approach we assume that the contribution from the hot stellar source can be neglected within the optical. We thus consider contributions only from the nebula and the cool giant, which simplifies Eq. (1) to $F_\lambda = F_\lambda^{nebula} + F_\lambda^{giant}$. This assumption can be applied for systems during quiescent phases, while during active phases, it is valid only under specific conditions. In the following two points we summarize reasons and conditions, under which this assumption can be applied.

(i) During quiescent phases the hot star contribution can be neglected in the optical, because of its very high temperature, which moves the maximum of its radiation to the extreme ultraviolet or supersoft X-ray domain, while the optical is contributed only with a very faint Rayleigh-Jeans tail in a blackbody approximation (e.g. Kenyon & Webbink, 1984; Mürset et al., 1991; Skopal, 2005). We investigated this case for three classical symbiotic stars AG Dra, AG Peg and Z And during their quiescent phases.

(ii) During active phases, a large optically thick disk is created around the accretor at the orbital plane. Its signatures are indicated best for the systems with a high orbital inclination (see Fig. 27 of Skopal, 2005). For the eclipsing symbiotics the hot stellar source is represented by a relatively warm ($T_\mathrm{h} \sim 22\,000$ K) disk's rim, which light contribution can be significant within the optical region. Therefore, the radiation from the hot active object can be neglected only during the eclipses. As example here, we analysed the light from the 1994 eclipse of AX Per during its 1989-95 active phase. In the case of non-eclipsing systems, the optical light from the hot object can be neglected at any orbital phase, because we are viewing the active hot star more from its pole, and thus its radiation is not cooled by the disk material on the line of sight. We demonstrate this case on example of AG Dra.

Finally, we note that our method is applicable to any object, whose continuous spectrum consists of two or one (nebular) component of radiation. We demonstrate this case on examples of symbiotic novae RR Tel, V1016 Cyg and a classical nova V1974 Cyg during its nebular phase.

2.2. The true continuum from UBV magnitudes

Photometric measurements i.e. observed *UBV* magnitudes used in this work are summarized in Table 2.

First, we corrected the observed magnitudes for the interstellar extinction using the extinction curve of Cardelli, Clayton & Mathis (1989) with appropriate E_{B-V} colour excess (Table 1). Second, to determine the true continuum using the multicolour photometry, we corrected the dereddened magnitudes for the influence of emission lines. For the purpose of this paper we used corrections presented by Skopal (2007), if not specified otherwise. The corrections are summarized in Table 3.

Table 1: Colour excesses, distances and spectral types of the giants.

Object	E_{B-V} [mag]	d [kpc]	Spectral type	ref.
AX Per	0.27	1.73	M4.5	1,7
AG Dra	0.08	1.1	K2(K4)	1,7
AG Peg	0.10	0.80	M3	1,7
Z And	0.30	1.5	M4.5	1,7
RR Tel	0.10	2.5	M6	2,3,7
V1016 Cyg	0.28	2.93	M7	4,5,7
V1974 Cyg	0.32	1.77	-	6

References:

1 - Skopal (2005) and references therein

2 - Penston (1983)

3 - Whitelock (1987)

4 - Nussbaumer & Schild (1981)

5 - Parimucha (2003)

6 - Chochol et al. (1993)

7 - Mürset & Schmid (1999)

Finally, according to the Pogson's equation, we converted the magnitudes of the true continuum, m_λ, to fluxes by

$$F_\lambda = 10^{-0.4(m_\lambda + q_\lambda)}, \tag{2}$$

where the constant q_λ defines the magnitude zero. For the standard Johnson *UBV* photometric system and the fluxes in units of erg cm^{-2} s^{-1} Å^{-1}, $q_\mathrm{U} = 20.9$ mag, $q_\mathrm{B} = 20.36$ mag and $q_\mathrm{V} = 21.02$ mag (e.g. Henden & Kaitchuck, 1982).

2.3. Contributions from the nebula and the giant

Now, let us have a look on basic relations for the nebular continuum and that from the giant. The nebular flux in Eq. (1) can be approximated by

$$F_\lambda^{nebula} = k_\mathrm{n} \times \varepsilon_\lambda(T_\mathrm{e}), \tag{3}$$

where k_n [cm^{-5}] is the scaling factor, which determines amount of the nebula and $\varepsilon_\lambda(T_\mathrm{e})$ is the volume emission coefficient [erg cm^3 s^{-1} Å^{-1}], which depends on the electron temperature of the nebula T_e, and is a function of the wavelength (e.g. Brown & Mathe 1970). For the sake of simplicity, we calculated the volume emission coefficient for the hydrogen plasma only, including contributions from recombination and bremsstrahlung. In addition, Eq. (3) requires T_e, and thus the emission coefficient $\varepsilon_\lambda(T_\mathrm{e})$, to be constant throughout the nebula. The total emission produced by the optically thin nebula is

$$4\pi d^2 F_\lambda^{nebula} = \varepsilon_\lambda \int_V n_\mathrm{e} n_+ \mathrm{d}V = \varepsilon_\lambda EM, \tag{4}$$

where EM [cm^{-3}] is the so-called emission measure. It is determined by the volume of the nebula and concentrations of electrons and ions (protons), n_e and n_+, respectively. So, with the

Table 2: Input parameters for investigated objects - Photometric measurements.

Object	Julian date $JD-24...$	U [mag]	B [mag]	V [mag]
AX Per	49 571	12.689	12.873	11.583
	49 575	12.712	12.895	11.641
	49 593	12.744	12.946	11.790
	49 601	12.733	12.936	11.681
	49 608	12.742	12.999	11.722
	49 621	12.715	12.870	11.660
AG Dra	52 765	10.957	11.029	9.735
	53 178	10.952	11.044	9.720
	52 919	9.189	10.022	9.181
AG Peg	49 974	9.16	9.76	8.56
	49 988	9.13	9.73	8.55
	49 993	9.09	9.71	8.55
	49 996	9.10	9.76	8.58
	50 012	8.97	9.75	8.56
	50 024	9.08	9.69	8.56
Z And	45 172	11.41	11.72	10.50
	45 195	11.28	11.74	10.64
	45 196	11.27	11.77	10.64
	45 204	11.24	11.77	10.67
RR Tel	48 066	9.90	11.26	10.84
	48 067	9.83	11.24	10.84
V1016 Cyg	45 975	10.26	11.41	11.15
V1974 Cyg	48 883	8.243	9.359	9.426

Table 3: Input parameters - Corrections for the emission lines.

Object	Julian date $JD-24...$	ΔU [mag]	ΔB [mag]	ΔV [mag]
AX Per	49 600	-0.77	-0.62	-0.19
AG Dra	52 765	-0.033	-0.10	-0.01
	53 172	-0.030	-0.08	-0.01
	52 919	-0.081	-0.12	-0.02
AG Peg	49 305	-0.19	-0.41	-0.12
Z And	45 293	-0.30	-0.48	-0.12
RR Tel	51 836	-1.71	-1.68	-0.87
V1016 Cyg	46 045	-1.23	-1.67	-1.19
V1974 Cyg	48 883	-1.57	-1.73	-0.66

aid of Eq. (3), the emission measure can be expressed as

$$EM = 4\pi d^2 k_n = 4\pi d^2 \frac{F_\lambda^{nebula}}{\varepsilon_\lambda(T_\mathrm{e})}, \tag{5}$$

where d is the distance to the object.

Due to the asymmetry of the U filter with respect to the wavelength of the Balmer discontinuity, λ_Balmer, we calculated the emission coefficient ε_U as the weighted average of its values from both sides of the Balmer jump (see Skopal, 2009). For the response function of the U filter, as published by Matthews & Sandage (1963), we get

$$\varepsilon_\mathrm{U} \doteq 0.6\,\varepsilon_{\mathrm{U}^-} + 0.4\,\varepsilon_{\mathrm{U}^+}, \tag{6}$$

where $\varepsilon_{\mathrm{U}^-}$ and $\varepsilon_{\mathrm{U}^+}$ are emission coefficients at the short and long wavelength side of the λ_Balmer, respectively.

The stellar radiation from cool giants of different spectral types can be characterized by different colour indices. For the purpose of this work we used colour indices from Johnson (1966). To simplify relations introduced in the following section, we denote the colour indices of the giant's spectrum, $U-B$ and $B-V$, by UB and BV, respectively.

2.4. Parameters of the nebula and giant

Here we propose a method to estimate parameters of the nebular radiation (T_e, EM) and that of the giant (e.g. V^{giant}), which dominates the optical part of the spectrum of most symbiotic stars. Based on the assumptions formulated in Sect. 2.1. and relations for the nebular emission (Sect. 2.3.), we can write following set of equations for the considered components of radiation. First, the total flux in the continuum is given by the superposition of fluxes from the nebula and the cool giant, i.e.

$$F_\mathrm{U}^{nebula} + F_\mathrm{U}^{giant} = 10^{-0.4(U^{cont}+q_\mathrm{U})}, \tag{7}$$

$$F_\mathrm{B}^{nebula} + F_\mathrm{B}^{giant} = 10^{-0.4(B^{cont}+q_\mathrm{B})}, \tag{8}$$

$$F_\mathrm{V}^{nebula} + F_\mathrm{V}^{giant} = 10^{-0.4(V^{cont}+q_\mathrm{V})}, \tag{9}$$

where U^{cont}, B^{cont} and V^{cont} are magnitudes of the true continuum (Sect. 2.2.). Second, according to Eq. (3), the nebular flux in the spectrum is a function of the scaling factor k_n and the electron temperature T_e, i.e.

$$F_\mathrm{U}^{nebula} = k_\mathrm{n}\,\varepsilon_\mathrm{U}(T_\mathrm{e}), \tag{10}$$

$$F_\mathrm{B}^{nebula} = k_\mathrm{n}\,\varepsilon_\mathrm{B}(T_\mathrm{e}), \tag{11}$$

$$F_\mathrm{V}^{nebula} = k_\mathrm{n}\,\varepsilon_\mathrm{V}(T_\mathrm{e}). \tag{12}$$

Third, the ratio of the fluxes from the giant in different filters can be expressed with the aid of the Pogson's equation as

$$\frac{F_\mathrm{U}^{giant}}{F_\mathrm{B}^{giant}} = 10^{-0.4(U^{giant}-B^{giant}+q_\mathrm{U}-q_\mathrm{B})} = 10^{-0.4(UB+q_\mathrm{U}-q_\mathrm{B})}, \tag{13}$$

$$\frac{F_\mathrm{B}^{giant}}{F_\mathrm{V}^{giant}} = 10^{-0.4(B^{giant}-V^{giant}+q_\mathrm{B}-q_\mathrm{V})} = 10^{-0.4(BV+q_\mathrm{B}-q_\mathrm{V})}. \tag{14}$$

Thus we have a system of eight equations (Eqs. (7) to (14)) for eight variables,

$$F_\mathrm{U}^{nebula},\ F_\mathrm{B}^{nebula},\ F_\mathrm{V}^{nebula},\ F_\mathrm{U}^{giant},\ F_\mathrm{B}^{giant},\ F_\mathrm{V}^{giant},\ k_\mathrm{n} \text{ and } T_\mathrm{e},$$

which can be solved for the known spectral type of the cool giant (i.e. the $U-B$ and $B-V$ indices) and the measured UBV magnitudes. The aim is to determine the three fundamental parameters, the electron temperature T_e, the scaling factor k_n and the giant's magnitude, V^{giant}. The first two parameters determine the nebular emission, while the third one settles the radiation from the giant characterized with indices $U-B$ and $B-V$, and thus defines the second term on the right side of Eq. (1). From the abovementioned system of equations (Eqs. (7) to (14)) we can derive a relation for determining the electron temperature in a form (see Appendix A)

$$\begin{aligned}&\frac{\varepsilon_\mathrm{B}(T_\mathrm{e})}{\varepsilon_\mathrm{V}(T_\mathrm{e})}\left[10^{-0.4(V^{cont}+UB-q_\mathrm{B})} - 10^{-0.4(U^{cont}-BV-q_\mathrm{B})}\right] + \\ &+ \frac{\varepsilon_\mathrm{U}(T_\mathrm{e})}{\varepsilon_\mathrm{V}(T_\mathrm{e})}\left[10^{-0.4(B^{cont}-BV-q_\mathrm{U})} - 10^{-0.4(V^{cont}-q_\mathrm{U})}\right] + \\ &+ \left[10^{-0.4(U^{cont}-q_\mathrm{V})} - 10^{-0.4(B^{cont}+UB-q_\mathrm{V})}\right] = 0.\end{aligned} \tag{15}$$

Solving this equation for T_e, allows us to determine easily other parameters. For example, the scaling factor k_n as

$$k_n = \frac{F_V^{nebula}}{\varepsilon_V(T_e)} = \frac{10^{-0.4(BV+V^{cont}+q_B)} - 10^{-0.4(B^{cont}+q_B)}}{10^{-0.4(BV+q_B-q_V)}\varepsilon_V(T_e) - \varepsilon_B(T_e)} \quad (16)$$

and the giant's magnitude in the V passband V^{giant} as

$$V^{giant} = -2.5\log\left[10^{-0.4(V^{cont}+q_V)} - F_V^{nebula}\right] - q_V, \quad (17)$$

where F_V^{nebula} is given by

$$F_V^{nebula} = \frac{10^{-0.4(BV+V^{cont}+q_B)} - 10^{-0.4(B^{cont}+q_B)}}{10^{-0.4(BV+q_B-q_V)} - \frac{\varepsilon_B(T_e)}{\varepsilon_V(T_e)}}. \quad (18)$$

For more details see Appendix A. The ratios of the emission coefficients $\varepsilon_U/\varepsilon_V$ and $\varepsilon_B/\varepsilon_V$ are plotted in Fig. 1.

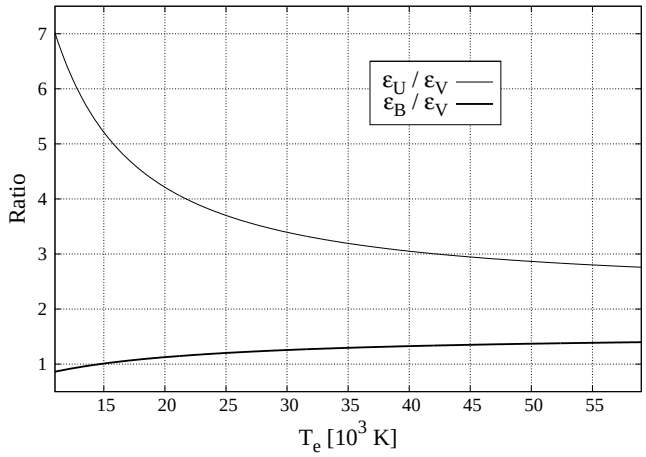

Figure 1: Ratios of the emission coefficients we used to solve Eq. (15).

3. Application to selected symbiotic stars

Our resulting parameters, the electron temperature T_e (from Eq. (15)), scaling factor k_n (Eqs. (3) and (16)), emission measure EM (see Eq. (5)) and the V magnitude of the giant V^{giant} (Eq. (17)) are summarized in Table 4. Values of EM were scaled for distances summarized in Table 1. Disentangled UBV magnitudes for the investigated objects are plotted in Fig. 2.

Assuming that the uncertainties of the observed U, B and V magnitudes for all investigated systems are ±0.05 mag, ±0.03 mag and ±0.03 mag, respectively (e.g. Skopal et al., 2007), we derived intervals of possible values of the searched parameters, which can be found in the fourth, sixth, eighth and tenth column in Table 4. Uncertainties in the corrections for emission lines are not included. If more photometric measurements were available, we used mean values of parameters, corrensponding to the individual UBV magnitudes. For these cases, we adopted uncertainties as the interception of parameter ranges given by individual measurements (except for the brightness of the cool giant in Z And and AX Per where we took the mean values of upper and lower limit of intervals because those interceptions were empty). Investigated objects are discussed in detail in the following subsections.

3.1. Classical symbiotic stars during quiescent phase

3.1.1. AG Dra

AG Dra is a yellow symbiotic star, because its cool component was classified as a normal K2 giant (e.g. Mürset & Schmid, 1999). To analyse a quiescent phase of AG Dra by our method, we used U, B, V measurements made on 2003/05/05 (Skopal et al., 2004) and 2004/06/21 (Skopal et al., 2007). We selected these dates, because of having simultaneous spectroscopic observations, which allowed us to determine corrections for emission lines on the UBV magnitudes (Fig. 6 of González-Riestra et al., 2008, and Viotti, private communication). The colour indices for a K2 giant, $B-V = 1.16$ and $U-B = 1.16$ (Johnson, 1966) are, however, in conflict with the observed indices of true continuum, $(B-V)_{obs} \doteq 1.3$ and $(U-B)_{obs} \doteq -0.2$, because observations contain contributions from both the giant and the nebula. Therefore, for the purpose of our analysis we adopted the giant's spectral type of K4, which is characterized with indices $B-V = 1.41$ and $U-B = 1.66$ (Johnson, 1966).

Applying our method (Eqs. (15) to (17)) to these data we obtained the electron temperature of the nebula, $T_e \approx 20\,000$ K and its emission measure, $EM \sim 1.7 \times 10^{59}$ cm^{-3}.

3.1.2. AG Peg

AG Peg is known as the slowest symbiotic nova. Currently, it displays all signatures of a classical symbiotic star in a quiescent phase (Kenyon et al., 1993; Mürset & Nussbaumer, 1994). We investigated AG Peg around its optical maximum in 1993 November, at the orbital phase $\varphi = 0.63$. Selection of these photometric data was important to compare our results with another analysis and to use appropriate corrections for emission lines (see Skopal, 2007). The U, B, V magnitudes were taken from Tomov & Tomova (1998). We used values of 6 measurements obtained between JD 2 449 974.3 and JD 2 450 024.3 and then averaged our results obtained from individual nights. For the spectral type of the giant in AG Peg we adopted M3 (Mürset & Schmid, 1999).

Analyzing these data we revealed $T_e \sim 17\,910$ K and $EM \sim 4.85 \times 10^{59}$ cm^{-3}, which are quite similar to those obtained by Skopal (2005).

3.1.3. Z And

Z And is a prototype of the class of symbiotic stars. We analysed U, B, V measurements taken around a light maximum of a quiescent phase (i.e. $\varphi \sim 0.5$), because the corrections for emission lines were made at the same orbital position of the binary. For the purpose of our analysis, we used U, B, V magnitudes taken by Belyakina (1992). We selected 4 measurements from JD ~ 2 445 171.51 to JD ~ 2 445 204.42. The spectral type of the giant in Z And is M4.5 (Mürset & Schmid, 1999). However, the giant's colour indices are available only for spectral types of M4 and/or M5. Therefore, we used indices for a M4

and M5 giant separately, and then averaged our results obtained from individual nights.

Our resulting temperature, $T_e \sim 29\,300$ K, is somewhat higher than that determined by Skopal (2005). Using indices of a M5 giant led to a lower temperature, $T_e \sim 28\,390$ K, while indices for a M4 giant yielded $T_e \sim 30\,220$ K. Our emission measure, $EM \sim 7.8 \times 10^{59}$ cm^{-3}, is quite similar to that determined independently (Skopal, 2005).

3.2. Classical symbiotic stars during active phase

3.2.1. AX Per

AX Per is known as eclipsing symbiotic binary with an orbital period of 680 days (Skopal, 1991). The cool component of the binary is a normal giant of the spectral type M4.5 (Mürset & Schmid, 1999). During active phases we observe narrow minima in the light curve at the position of the inferior conjunction of the giant. It is believed that they are caused by eclipses of the hot object by the cool giant.

In this paper we studied the 1994 eclipse, observed during the 1989-95 active phase of AX Per. We used 6 *UBV* measurements from the totality, between JD 2 449 570.54 and JD 2 449 620.56 (Skopal et al., 1995). We assumed that contributions from both the nebula and the giant had not been varying significantly during the relatively short time of the total eclipse ($\sim$ 2 months). Therefore, also in this case, we derived parameters for each night set of *UBV* magnitudes, and then used their means, to get the most probable values of the fitting parameters. As in the case of Z And we applied our method to both spectral types of a giant, M4 and M5, and used their means to obtain resulting parameters.

In this way we received the electron temperature of the nebula $T_e \sim 30\,770$ K, the scaling factor, $k_n \sim 0.41 \times 10^{15}$ cm^{-5} which corresponds to the emission measure, $EM \sim 1.47 \times 10^{59}$ cm^{-3}. Using the giant of the spectral type M5 led to lower values of both nebular parameters than for a M4 giant. Skopal (2005) modelled the UV–IR SED from the 1990 eclipse and found very similar value of T_e, but a factor of $\sim$2 higher EM than we obtained for the 1994 eclipse. The lower amount of the nebular emission indicated during the 1994 eclipse is probably connected with the ending of the 1989-95 active phase. Note that the high temperature nebula appears to be strong just during active phases of symbiotic stars (Skopal, 2005). Finally, the mean value of the giant's V magnitude is 11.15 mag. However, its value runs from 11.02 to 11.30 mag for these 6 individual *UBV* measurements, including their uncertainties. Different values of the V^{giant} magnitudes are beyond the measured uncertainties. Therefore, we conclude that they can be caused by a variable brightness of the giant during the eclipse, perhaps due to its pulsations.

3.2.2. AG Dra

Here we demonstrate our method on the *UBV* magnitudes measured during the optical burst of AG Dra in 2003 October (see Fig. 8 in Skopal et al., 2007). We derived $T_e \approx 45\,000$ K and $EM \sim 1.9 \times 10^{60}$ cm^{-3}, which are significantly higher than those we indicated during quiescent phase. To check sensitivity of these parameters to the contribution from the giant, we used different colour indices of the giant. By this way we obtained a lower $T_e \sim 30\,000$ K and 38 000 K for a K2 and K3 giant, respectively. However, the emission measure was rather insensitive to such a small change in the spectral type of the giant, because of its large quantity. We note that during active phases the emission measure of the symbiotic nebula in AG Dra increased by a factor of $\sim$10.

In both cases (quiescence and activity) our parameters were in a good agreement with those obtained independently by a precise modelling the $(0.12 - 5)\,\mu$m SED in the continuum (see Fig. 13 of Skopal, 2005).

3.3. Symbiotic novae

3.3.1. RR Tel

RR Tel is a slow symbiotic nova that underwent an outburst in 1944 and whose optical light curve is still fading (Mürset & Nussbaume 1994; Kotnik-Karuza et al., 2006). The binary contains a Mira-type variable as the cool component, which produces a massive wind and give rise to a strong dust emission (e.g Jurkič & Kotnik-Karuza, 2007; Angeloni et al., 2007). The system contains a very hot and luminous white dwarf (Mürset & Nussbaumer, 1994), which ionizes a fraction of the giant's wind resulting in a strong nebular emission in the spectrum of RR Tel (Bryan & Kwok, 1991).

For the spectral type of the giant in RR Tel we adopted M6 (Mürset & Schmid, 1999). We applied our method of disentangling the *UBV* magnitudes to the measurements made on 1990/06/23 and 1990/06/24 as published by Munari et al. (1992). We found the electron temperature and the emission measure that are typical for the quiescent phases of other symbiotic stars (Table 4).

3.3.2. V1016 Cyg

V1016 Cyg underwent its nova-like outburst in 1964 (Fitzgerald et al. 1966). The binary contains a Mira variable as the cool component with a strong IR dust emission (e.g. Taranova and Shenavrin, 2000; Parimucha et al., 2002; Archipova et al., 2008). The spectral type of the giant in V1016 Cyg is M7 (Mürset & Schmid, 1999). However, Johnson (1966) doesn't provide the indices for this spectral type. Therefore, firstly we used the spectral type M6, and secondly, we neglected the giant contribution to *UBV* magnitudes, at all. We found that there is no significant difference between these two possibilities. As a giant of the spectral type M7 is even cooler than that of the M6 type (i.e. its contribution to the optical is lower), we decided to neglect the giant contribution and calculated only the nebular continuum. Also, it is important to note that the nebular contribution dominates the optical (see Fig. 5 of Skopal, 2007), which makes it difficult to extract the relatively very faint light from the giant by our method. In our analysis we used *UBV* measurements published by Parimucha et al. (2000) from 1984 October, which are close to dates of the spectroscopic observations used for emission lines corrections. The large emission measure, $EM \sim 10^{60}$ cm^{-3}, is typical for the active symbiotic systems.

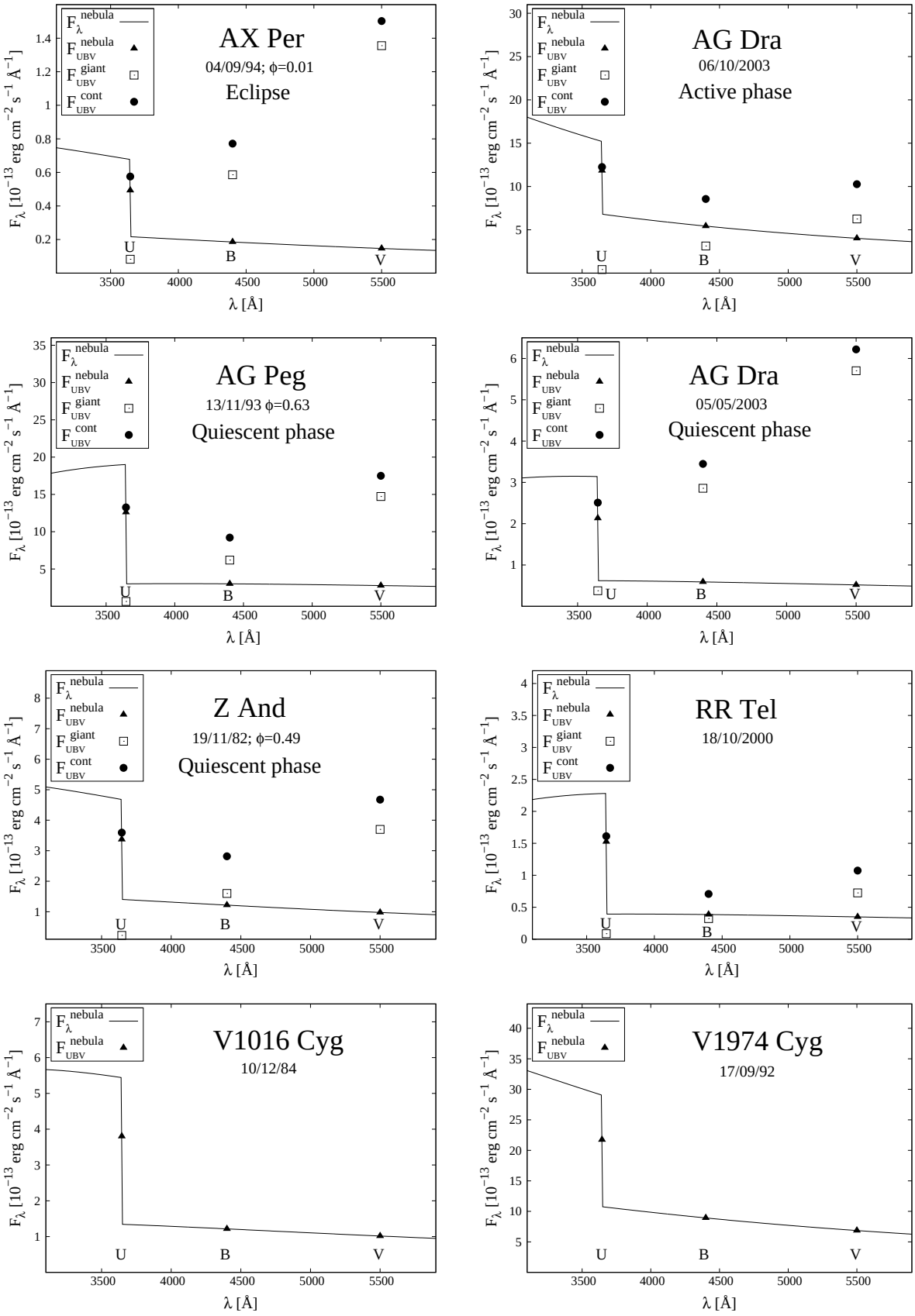

Figure 2: The *UBV* SED for investigated symbiotic binaries and novae. The *UBV* fluxes in the continuum, $F^{cont}_{\rm UBV}$ (Sect. 2.2), and their disentangled components from nebula, $F^{nebula}_{\rm UBV}$, and the giant, $F^{giant}_{\rm UBV}$, are denoted by symbols in the legend. The nebular continuum, F^{nebula}_{λ}, is drawn with a solid line.

Table 4: Physical parameters of the nebula and the giant for selected symbiotic stars and novae obtained by our method of disentangling their UBV magnitudes.

Object	Julian date $JD-2\,4...$	T_e [K]	$T_{e,min}$ - $T_{e.max}$ [K]	k_n [10^{15} cm^{-5}]	$k_{n,min}$ - $k_{n,max}$ [10^{15} cm^{-5}]	EM [10^{59} cm^{-3}]	EM_{min} - EM_{max} [10^{59} cm^{-3}]	V^{giant} [mag]	V^{giant}_{min} - V^{giant}_{max} [mag]	ph.*
AX Per	49 600	30 770	27 600 - 37 600	0.41	0.39 - 0.47	1.47	1.40 - 1.68	11.15	11.08 - 11.20	A,E
AG Dra	52 765	20 710	12 330 - 35 410	1.24	0.70 - 1.90	1.80	1.02 - 2.75	9.59	9.53 - 9.66	Q
	53 172	19 230	11 200 - 32 610	1.16	0.62 - 1.79	1.68	0.90 - 2.59	9.57	9.50 - 9.64	Q
	52 919	44 940	34 210 - 64 160	13.2	11.2 - 16.1	19.1	16.2 - 23.3	9.49	9.39 - 9.61	A
AG Peg	49 305	17 910	16 500 - 19 130	6.33	6.00 - 6.93	4.85	4.60 - 5.30	8.56	8.51 - 8.60	Q
Z And	45 293	29 300	24 370 - 38 040	2.89	2.59 - 3.14	7.78	6.99 - 8.45	10.08	10.01 - 10.16	Q
RR Tel	51 836	18 910	16 370 - 21 860	0.81	0.73 - 0.88	6.02	5.44 - 6.60	11.83	11.74 - 11.90	Q
V1016 Cyg	46 045	24 480	22 100 - 26 530	2.59	2.52 - 2.71	26.6	25.8 - 27.9	-	-	Q
V1974 Cyg	48 883	35 760	31 480 - 41 420	20.4	19.3 - 21.8	76.5	72.3 - 81.8	-	-	Q

* phase: active phase (A), eclipse (E), quiescent phase (Q)

3.4. Classical nova V1974 Cyg

V1974 Cyg (Nova Cygni 1992) belongs to the group of the classical novae. It was discovered by Collins (1992) on 1992, February 19. To investigate the physical conditions in this nova by our method, we used the data from its nebular phase taken around day 210 after the optical maximum. According to the X-ray light curve of V1974 Cyg (see Fig. 1 of Krautter et al., 1996), the burning white dwarf in the nova was already very hot at that time. Therefore we could neglect its contribution to the optical as well as that from the red dwarf companion. The optical spectrum was thus strongly dominated by the nebular radiation. As a result, we derived parameters characterizing the nebular radiation component only. For this purpose, we used two flux-points corresponding, for example, to U and B magnitudes. Particularly, we used photometric measurements taken at JD 2 448 883.4 (1992/09/17) as published by Chochol et al. (1993).

Disentangling these U and B measurements, we found a relatively high electron temperature of $T_{\rm e} \sim 36\,000$ K, and also a very high emission measure, $EM \sim 8 \times 10^{60}$ cm^{-3} (Table 4).

4. Discussion

Physical parameters for the symbiotic nebulae, which we derived by disentangling the UBV measurements (Sect. 3, Table 4), are in a good agreement with those determined by a precise modelling the UV–IR SED (Skopal, 2005). We found that the emission measure can be determined with a higher accuracy than the electron temperature of the nebula. The former is given by scaling the emission coefficient, and thus can be estimated within the uncertainty of the photometric measurements, while the latter is given by the profile of the volume emission coefficient. In addition, for lower values of electron temperatures, to say $T_{\rm e} < 25\,000$ K, the profile is relatively steeper than for higher values of $T_{\rm e}$. As a result a lower $T_{\rm e}$ can be determined with a better accuracy than a higher one, and vice versa. Taking into account difference in $T_{\rm e}$ between quiescent and active phases, we can, in general, conclude that during the quiescence, $T_{\rm e}$ can be determined more precisely than in the activity, in spite of equal uncertainties of UBV measurements.

Parameters of the nebula in our model also depend on colour indices of the cool giant, which values, however, are often different in different articles. For the purpose of this work we adopted indices from Johnson (1966). Further, it is important to know the correct spectral type of the giant. Also here different authors recommend slightly different spectral types for the giants in the investigated systems. Furthermore, our analysis revealed that the brightness of the cool giants can vary within a few times 0.1 mag (e.g. AX Per during the 1994 eclipse). This type of variability can be ascribed to pulsations of late-type giants, because they represent their typical behaviour. All these uncertainties cannot be included in our analysis. Therefore, our resulting magnitudes of the giant can be considered only as estimates of their mean values.

It is of importance to note that we modelled just the optical continuum. So it is inevitable to know corrections for the influence of emission lines on the UBV magnitudes. Uncertainty (ignorance) of these corrections can represent a significant source of errors of the fitting parameters.

Knowing actual colour indices of the giant and corrections for emission lines, our system of equations allowed us to study the effect of uncertainties of the UBV magnitudes to the fitting parameters. We could easily found extreme values of the parameters, as well as their values based on all possible combinations of UBV magnitudes.

During quiescent phases we found the electron temperature $T_e \sim 20\,000\,K$, while during active phases our method indicated higher values of $T_e \sim 30\,000 - 40\,000$ K. During quiescence the emission measure was in the order of $\sim 10^{59}$ cm^{-3}, while during activity we identified its increase to $\sim 10^{60}$ cm^{-3}. For symbiotic novae we obtained even higher values of $\sim 10^{60} - 10^{61}$ cm^{-3}.

Finally, we note that our method of disentangling the UBV magnitudes can be applied to any spectrum composed from a nebular and stellar component of radiation.

5. Conclusion

In this contribution we employed a method of disentangling the composite spectrum of the optical continuum on the basis of simple multicolour photometric measurements. Our method (Sect. 2) allowed us to determine the physical parameters of the

main contributing components of the radiation into the optical region – the nebula and the giant. Main results may be summarized as follows.

(i) On the basis of the *UBV* photometric measurements, we determined the true optical continuum of the selected symbiotic (-like) binaries.

(ii) We compared the observed continuum by a model, which includes contributions from the nebula and the giant (Sect. 3). In this way we determined the electron temperature and emission measure of the nebula, and the *V* magnitude of the giant.

(iii) Our model parameters are well comparable with those determined independently by another method. In particular, by a precise modelling the UV–IR SED as introduced by Skopal (2005).

(iv) Our approach thus provides a good estimate of the physical parameters of contributing sources of radiation into the optical on the basis of a simple *UBV* photometry.

Acknowledgment

This research was supported by a grant of the Slovak Academy of Sciences, VEGA No. 2/0038/10.

Appendix A. Relation for determining the electron temperature

In this appendix we derive relation for determining the electron temperature (Eq. 15) from the following system of equations

$$F_{\rm U}^{giant} + F_{\rm U}^{nebula} = 10^{-0.4(U^{cont}+q_{\rm U})}, \quad (A.1)$$

$$F_{\rm B}^{giant} + F_{\rm B}^{nebula} = 10^{-0.4(B^{cont}+q_{\rm B})}, \quad (A.2)$$

$$F_{\rm V}^{giant} + F_{\rm V}^{nebula} = 10^{-0.4(V^{cont}+q_{\rm V})}, \quad (A.3)$$

$$F_{\rm U}^{nebula} = k_{\rm n}\,\varepsilon_{\rm U}(T_{\rm e}), \quad (A.4)$$

$$F_{\rm B}^{nebula} = k_{\rm n}\,\varepsilon_{\rm B}(T_{\rm e}), \quad (A.5)$$

$$F_{\rm V}^{nebula} = k_{\rm n}\,\varepsilon_{\rm V}(T_{\rm e}), \quad (A.6)$$

$$\frac{F_{\rm U}^{giant}}{F_{\rm B}^{giant}} = 10^{-0.4(U^{giant}-B^{giant}+q_{\rm U}-q_{\rm B})} = 10^{-0.4(UB+q_{\rm U}-q_{\rm B})}, \quad (A.7)$$

$$\frac{F_{\rm B}^{giant}}{F_{\rm V}^{giant}} = 10^{-0.4(B^{giant}-V^{giant}+q_{\rm B}-q_{\rm V})} = 10^{-0.4(BV+q_{\rm B}-q_{\rm V})}. \quad (A.8)$$

At the beginning we have 8 equations (A.1 - A.8).
We express the flux from the giant in the *V* passband $F_{\rm V}^{giant}$ from Eq. (A.3) as

$$\boxed{F_{\rm V}^{giant} = 10^{-0.4(V^{cont}+q_{\rm V})} - F_{\rm V}^{nebula}}$$

and substitute it to the remaining equations. Equations (A.1), (A.2), (A.4), (A.5), (A.6), (A.7) do not change. The Eq. (A.8) turns into

$$F_{\rm B}^{giant} = 10^{-0.4(BV+V^{cont}+q_{\rm B})} - 10^{-0.4(BV+q_{\rm B}-q_{\rm V})}F_{\rm V}^{nebula}. \quad (A.9)$$

We have 7 equations now (A.1, A.2, A.4, A.5, A.6, A.7, A.9).
Further, we express the flux from the giant in the *B* passband $F_{\rm B}^{giant}$ from Eq. (A.2) as

$$\boxed{F_{\rm B}^{giant} = 10^{-0.4(B^{cont}+q_{\rm B})} - F_{\rm B}^{nebula}}$$

and substitute it to remaining equations. Equations (A.1), (A.4), (A.5), (A.6) don't change. The Eq. (A.7) turns into

$$F_{\rm U}^{giant} = 10^{-0.4(UB+B^{cont}+q_{\rm U})} - 10^{-0.4(UB+q_{\rm U}-q_{\rm B})}F_{\rm B}^{nebula}. \quad (A.10)$$

The Eq. (A.9) turns into

$$10^{-0.4(B^{cont}+q_{\rm B})} - F_{\rm B}^{nebula} = \\ = 10^{-0.4(BV+V^{cont}+q_{\rm B})} - 10^{-0.4(BV+q_{\rm B}-q_{\rm V})}F_{\rm V}^{nebula}. \quad (A.11)$$

We have 6 equations now (A.1, A.4, A.5, A.6, A.10, A.11).
Further, we express the flux from the giant in the *U* passband $F_{\rm U}^{giant}$ from Eq. (A.1) as

$$\boxed{F_{\rm U}^{giant} = 10^{-0.4(U^{cont}+q_{\rm U})} - F_{\rm U}^{nebula}}$$

and substitute it to remaining equations. Equations (A.4), (A.5), (A.6), (A.11) don't change. The Eq. (A.10) turns into

$$10^{-0.4(U^{cont}+q_{\rm U})} - F_{\rm U}^{nebula} = \\ = 10^{-0.4(UB+B^{cont}+q_{\rm U})} - 10^{-0.4(UB+q_{\rm U}-q_{\rm B})}F_{\rm B}^{nebula}. \quad (A.12)$$

We have 5 equations now (A.4, A.5, A.6, A.11, A.12).
Further, we express the scaling factor of the nebula $k_{\rm n}$ from Eq. (A.4) as

$$\boxed{k_{\rm n} = \frac{F_{\rm U}^{nebula}}{\varepsilon_{\rm U}(T_{\rm e})}}$$

and substitute it to remaining equations. Equations (A.11), (A.12) don't change. The Eq. (A.5) turns into

$$F_{\rm B}^{nebula} = \frac{\varepsilon_{\rm B}(T_{\rm e})}{\varepsilon_{\rm U}(T_{\rm e})}F_{\rm U}^{nebula}. \quad (A.13)$$

The Eq. (A.6) turns into

$$F_{\rm V}^{nebula} = \frac{\varepsilon_{\rm V}(T_{\rm e})}{\varepsilon_{\rm U}(T_{\rm e})}F_{\rm U}^{nebula}. \quad (A.14)$$

We have 4 equations now (A.11, A.12, A.13, A.14).
Further, we express the flux from the nebula in the *U* passband $F_{\rm U}^{nebula}$ from Eq. (A.13) as

$$\boxed{F_{\rm U}^{nebula} = \frac{\varepsilon_{\rm U}(T_{\rm e})}{\varepsilon_{\rm B}(T_{\rm e})}F_{\rm B}^{nebula}}$$

and substitute it to remaining equations. Equation (A.11) doesn't change. The Eq. (A.14) turns into

$$F_{\rm V}^{nebula} = \frac{\varepsilon_{\rm V}(T_{\rm e})}{\varepsilon_{\rm B}(T_{\rm e})}F_{\rm B}^{nebula}. \quad (A.15)$$

The Eq. (A.12) turns into

$$10^{-0.4(U^{cont}+q_U)} - \frac{\varepsilon_U(T_e)}{\varepsilon_B(T_e)} F_B^{nebula} = \\ = 10^{-0.4(UB+B^{cont}+q_U)} - 10^{-0.4(UB+q_U-q_B)} F_B^{nebula}. \quad (A.16)$$

We have 3 equations now (A.11, A.15, A.16).
Further, we express the flux from the nebula in the B passband F_B^{nebula} from Eq. (A.15) as

$$\boxed{F_B^{nebula} = \frac{\varepsilon_B(T_e)}{\varepsilon_V(T_e)} F_V^{nebula}}$$

and substitute it to remaining equations. The Eq. (A.11) turns into

$$10^{-0.4(B^{cont}+q_B)} - \frac{\varepsilon_B(T_e)}{\varepsilon_V(T_e)} F_V^{nebula} = \\ = 10^{-0.4(BV+V^{cont}+q_B)} - 10^{-0.4(BV+q_B-q_V)} F_V^{nebula}. \quad (A.17)$$

The Eq. (A.16) turns into

$$10^{-0.4(U^{cont}+q_U)} - \frac{\varepsilon_U(T_e)}{\varepsilon_V(T_e)} F_V^{nebula} = \\ = 10^{-0.4(UB+B^{cont}+q_U)} - 10^{-0.4(UB+q_U-q_B)} \frac{\varepsilon_B(T_e)}{\varepsilon_V(T_e)} F_V^{nebula}. \quad (A.18)$$

We have 2 equations now (A.17, A.18).
Further, we eliminate the flux from the nebula in the V passband F_V^{nebula} from Eqs. (A.17) and (A.18). We get the following equation:

$$\boxed{F_V^{nebula} = \frac{10^{-0.4(BV+V^{cont}+q_B)} - 10^{-0.4(B^{cont}+q_B)}}{10^{-0.4(BV+q_B-q_V)} - \frac{\varepsilon_B(T_e)}{\varepsilon_V(T_e)}} = \\ = \frac{10^{-0.4(UB+B^{cont}+q_U)} - 10^{-0.4(U^{cont}+q_U)}}{10^{-0.4(UB+q_U-q_B)} \frac{\varepsilon_B(T_e)}{\varepsilon_V(T_e)} - \frac{\varepsilon_U(T_e)}{\varepsilon_V(T_e)}}} \quad (A.19)$$

When we multiply Eq. (A.19) by its denominators and do some other simple mathematical operations we get

$$\frac{\varepsilon_B(T_e)}{\varepsilon_V(T_e)} \left[10^{-0.4(UB+BV+V^{cont}+q_U)} - 10^{-0.4(U^{cont}+q_U)}\right] + \\ + \frac{\varepsilon_U(T_e)}{\varepsilon_V(T_e)} \left[10^{-0.4(B^{cont}+q_B)} - 10^{-0.4(BV+V^{cont}+q_B)}\right] + \\ + 10^{-0.4(BV+U^{cont}+q_U+q_B-q_V)} - 10^{-0.4(UB+BV+B^{cont}+q_U+q_B-q_V)} = 0$$

For the sake of simplicity we divide previous equation by $10^{-0.4(BV+q_U+q_B)}$. Finally we get the equation for determining the electron temperature in a form

$$\boxed{\frac{\varepsilon_B(T_e)}{\varepsilon_V(T_e)} \left[10^{-0.4(V^{cont}+UB-q_B)} - 10^{-0.4(U^{cont}-BV-q_B)}\right] + \\ + \frac{\varepsilon_U(T_e)}{\varepsilon_V(T_e)} \left[10^{-0.4(B^{cont}-BV-q_U)} - 10^{-0.4(V^{cont}-q_U)}\right] + \\ + \left[10^{-0.4(U^{cont}-q_V)} - 10^{-0.4(B^{cont}+UB-q_V)}\right] = 0,} \quad (A.20)$$

which we used in this work (Eq. (15) in the main text). After determining the temperature T_e from Eq. (A.20), we can easily determine other parameters, F_V^{nebula}, F_B^{nebula}, F_U^{nebula}, k_n, F_U^{giant}, F_B^{giant} and F_V^{giant}. For example, we can use equations in the frames. If we are interested only in three fundamental parameters (T_e, k_n and V^{giant}) it is better to determine the scaling factor of the nebula, k_n, from

$$k_n = \frac{F_V^{nebula}}{\varepsilon_V(T_e)} \quad (A.21)$$

as we did in the main text.

References

Angeloni, R., Contini, M., Ciroi, S., Rafanelli, P., 2007. AJ 134, 205.
Arkhipova, V. P., Esipov, V. F., Ikonnikova, N. P., & Komissarova, G. V., 2008. Astronomy Letters 34, 474.
Belyakina, T., S., 1992. Izv. Krymsk. Astrofiz. Obs. 84, 49.
Bryan, G. L. & Kwok, S., 1991. ApJ 368, 252.
Brown, R. L., & Mathews, W. G., 1970. ApJ 160, 939.
Cardelli, J. A., Clayton, G. C., & Mathis, J. S., 1989 ApJ 345, 245.
Collins, P., 1992. IAU Circ. No. 5454.
Fitzgerald, M. P., Houk, N., McCuskey, S. W., & Hoffleit, D., 1966. ApJ 144, 1135.
Henden, A. A., & Kaitchuck, R. H., 1982. Astronomical Photometry, Van Nostrand Reinhold Company, New York
Chochol, D., Hric, L., Urban, Z., et al., 1993 A&A 277, 103.
González-Riestra, R., Viotti, R. F., Iijima, T., Rossi, C., Montagni, F., Bernabei, S., Frasca, A., Skopal, A., 2008. A&A 481, 725.
Johnson, H. L., 1966. ARA&A 4, 193.
Jurkič, T., & Kotnik-Karuza, D., 2007. Baltic Astronomy 16, 76.
Kenyon, S. J., & Webbink, R. F., 1984. ApJ 279, 252.
Kenyon, S. J., Mikolajewska, J., Mikolajewski, M., Polidan, R. S., & Slovak, M. H., 1993. AJ 106, 1573.
Kotnik-Karuza, D., Friedjung, M., Whitelock, P. A., Marang, F., Exter, K., Keenan, F. P., Pollacco, D. L., 2006. A&A 452, 503.
Krautter, J., Ögelman, H., Starrfield, S., Wichmann, R., & Pfeffermann, E., 1996. ApJ 456, 788.
Matthews, T. A. Sandage, A. R., 1963. ApJ 138, 30.
Munari, U., Yudin, B., F., Taranova, O., G., et al., 1992. Astron. Astrophys. Suppl. Ser. 93, 383.
Mürset, U., Nussbaumer, H., Schmid, H. M., & Vogel, M., 1991. A&A 248, 458.
Mürset, U., & Nussbaumer, H., 1994. A&A, 282, 586.
Mürset, U., & Schmid, H., M., 1999. Astron. Astrophys. Suppl. Ser. 137, 473.
Nussbaumer, H., Schild, H., 1981. A&A 101, 118.
Parimucha, Š., Arkhipova, V., P., Chochol, D., et al., 2000. Contrib. Astron. Obs. Skalnaté Pleso 30, 99.
Parimucha, Š., Chochol, D., Pribulla, T., Buson, L. M., & Vittone, A. A., 2002. A&A 391, 999.
Parimucha, Š., 2003. Contrib. Astron. Obs. Skalnaté Pleso 33, 99.
Penston, M., V., Benvenuti, P., Cassatella, A., et al., 1983. MNRAS 202, 833.
Skopal, A., 1991. *IBVS* No. 3603.
Skopal, A., 2005. A&A 440, 995.
Skopal, A., 2007. New. Astron. 12, 597.
Skopal, A., 2009. New. Astron. 14, 336.
Skopal, A., Hric, L., Chochol, D., et al., 1995. Contrib. Astron. Obs. Skalnaté Pleso 25, 53.
Skopal, A., Pribulla, T., Vaňko, M., et al., 2004. Contrib. Astron. Obs. Skalnaté Pleso 34, 45.
Skopal, A., Vaňko, M., Pribulla, T., et al., 2007. Astron. Nachr. 328, 909.
Taranova, O.G., Shenavrin, V.I., 2000. Astron. Letters 26, 600.
Tomov, N., Tomova, M., 1998. IBVS 4574.
Whitelock, P., A., 1987. PASP 99, 573.